

**DYNAMICS OF FERROELECTRIC NANO CLUSTER IN BaTiO₃
OBSERVED AS A REAL TIME CORRELATION BETWEEN TWO
SOFT X-RAY LASER PULSES**

KAI JI

*Solid State Theory Division, Institute of Materials Structure Science,
KEK, Graduate University for Advanced Studies, and CREST JST
Oho 1-1, Tsukuba, Ibaraki 305-0801, Japan
jkai@post.kek.jp*

KAZUMICHI NAMIKAWA

*Department of Physics, Tokyo Gakugei University
Nukuikita 4-1-1, Koganei, Tokyo 184-8501, Japan*

HANG ZHENG

*Department of Physics, Shanghai Jiao Tong University
Shanghai 200030, China*

KEIICHIRO NASU

*Solid State Theory Division, Institute of Materials Structure Science,
KEK, Graduate University for Advanced Studies, and CREST JST
Oho 1-1, Tsukuba, Ibaraki 305-0801, Japan*

We carry out a theoretical investigation to clarify the dynamic property of photo-created nano-sized ferroelectric cluster observed in the paraelectric BaTiO₃ as a real time correlation of speckle pattern between two soft X-ray laser pulses, at just above the paraelectric-ferroelectric phase transition temperature. Based on a model with coupled soft X-ray photon and ferroelectric phonon mode, we study the time dependence of scattering probability by using a perturbative expansion approach. The cluster-associated phonon softening as well as central peak effects are well reproduced in the phonon spectral function via quantum Monte Carlo simulation. Besides, it is found that the time dependence of speckle correlation is determined by the relaxation dynamics of ferroelectric clusters. Near the transition point, cluster excitation is stable, leading to a long relaxation time. While, at high temperature, cluster structure is subject to the thermal fluctuation, ending up with a short relaxation time.

Keywords: Nonlinear optics; soft X-ray laser; nano cluster.

1. Introduction

Ferroelectricity refers to the ability of developing a spontaneous polarization (electric dipole moment) on decreasing temperature below Curie point (T_c). As a prototype of the ferroelectric perovskite compounds, barium titanate (BaTiO₃) undergoes a transition from paraelectric cubic to ferroelectric tetragonal phase at $T_c=395$ K. In addition to its extensive application in the technology such as non-volatile memory devices, capacitor applications and piezoelectric transducers due to its high

dielectric constant and switchable spontaneous polarization,¹ there is also an enduring interest in understanding the mechanism of paraelectric-ferroelectric phase transition in it. Although it is generally considered that the transition might be a classic displacive soft-mode type driven by the anharmonic lattice dynamics,^{2,3} recent studies have suggested an existence of order-disorder instability competing with the displacive transition^{4,5}, making this issue still controversial to date.

Direct observation on creation and evolution of ferroelectric cluster around T_c is of crucial importance for clarifying the nature of phase transition. However, conventional techniques, like neutron scattering,⁶ polarizing optical microscopy⁷ and scanning probe microscopy,⁸ can hardly detect the ultrafast transient status of dipole clusters. In contrast, diffraction speckle patterns of BaTiO₃ crystal measured by the soft X-ray laser has turned out to be an efficient way to elucidate the dynamics of domain structure.⁹⁻¹¹

Very recently, Namikawa¹² study the nano-sized polarization clusters in BaTiO₃ at just above T_c by the plasma-based X-ray laser speckle measurement. In this experiment, two consecutive coherent X-ray laser pulses of 160 Å with an adjustable time difference are generated by the Michelson type beam splitter. After the photo excitation by the first pulse, ferroelectric clusters of nano scale are created in the paraelectric BaTiO₃ and tends to be smeared out gradually due to the thermal fluctuation. This relaxation of cluster structure thus can be recorded in the speckle patterns of the second pulse as a function of its delay time from the first pulse, which is known as the speckle intensity correlation function. It has been found that near the T_c , this correlation follows an exponential decay process, *i.e.*, the intensity of speckle pattern declines as the delay time increases. Moreover, the decay rate also decreases upon approaching T_c , indicating a critical slowing down of the dipole relaxation time. Hence, by measuring the correlation between two soft X-ray laser pulses, the real time relaxation dynamics of polarization clusters in BaTiO₃ is clearly represented.

In this work, we examine the above-mentioned novel behaviors of ferroelectric cluster observed by Namikawa from a theoretical point of view, aiming to provide a basis for understanding the critical nature of BaTiO₃. Our calculation confirms that the relaxation of photo-created nano clusters plays an essential role in determining the delay time dependence of speckle correlation function. The remaining of present paper is organized as follows. In Sec. 2, the model Hamiltonian and theoretical treatment are put forward. In Sec. 3, our numerical results are discussed in comparison with the experimental discoveries. In Sec. 4, a summary with conclusion is presented finally.

2. Theoretical model and method

In order to describe the optical response of BaTiO₃ due to X-ray scattering, we design a theoretical model to incorporate the radiation field and ferroelectric dipole correlation as well as a weak interplay between them. As mentioned above, the phase

transition in BaTiO₃ is likely to be an admixture of displacive and order-disorder types. For this sake, we adopt a Krumhansl-Schrieffer type phonon mode¹³ to characterize the ferroelectric anharmonicity in BaTiO₃, for this model is suitable for describing the crossover between displacive and order-disorder phase transitions.¹⁴ In this scenario, our model Hamiltonian reads ($\hbar = 1$ and $k_B = 1$ throughout this paper):

$$\begin{aligned}
H &= H_p + H_f + H_{pf}, \\
H_p &= \sum_k \Omega_k a_k^\dagger a_k, \\
H_f &= \frac{\omega_0}{2} \sum_l \left(-\frac{\partial^2}{\partial Q_l^2} + Q_l^2 - c_4 Q_l^4 + c_6 Q_l^6 \right) - \frac{\omega_0 d_2}{2} \sum_{\langle l, l' \rangle} Q_l Q_{l'} \\
H_{pf} &= \frac{V}{N} \sum_{q, q', k} a_{k+\frac{q}{2}}^\dagger a_{k-\frac{q}{2}} Q_{q'-\frac{q}{2}} Q_{-q'-\frac{q}{2}}, \tag{2.1}
\end{aligned}$$

where a_k^\dagger (a_k) is the creation (annihilation) operator of a photon with a wave vector k and an energy Ω_k . Q_l is the coordinate operator for ionic displacement along the easy axis of BaTiO₃ at the site l with a dipole oscillatory frequency ω_0 . Q_q ($\equiv N^{-1/2} \sum_l e^{-iql} Q_l$) is its Fourier component for wave vector q . Without losing generalitivity, here we use a simple cubic lattice, and the total number of lattice site is N . H_f is the extended Krumhansl-Schrieffer model for phonon, where a sixth order term of Q_l is introduced to produce a triple-well potential, because the phase transition of BaTiO₃ is first order. Thus, the lattice dynamic properties are determined by the frequency ω_0 , temperature T , and dimensionless parameters c_4 , c_6 , d_2 . H_{pf} corresponds to a Raman type bi-linear coupling between the ferroelectric phonon mode and photons as the phonon mode has an even parity in the present case, and V is the coupling strength.

Since there are two photons involved in the scattering with crystal, the photon-phonon scattering probability can be written as,

$$\begin{aligned}
P(t) &= \sum_{k_1, k'_1} \langle \langle a_{k_0}(0) a_{k_1}^\dagger(\Delta) a_{k_0}(t) a_{k'_1}^\dagger(\Delta+t) \\
&\quad \times a_{k'_1}(\Delta+t) a_{k_0}^\dagger(t) a_{k_1}(\Delta) a_{k_0}^\dagger(0) \rangle \rangle, \tag{2.2}
\end{aligned}$$

where,

$$\langle \langle \dots \rangle \rangle = \text{Tr}(e^{-\beta H} \dots) / (e^{-\beta H}), \tag{2.3}$$

means the expectation, β ($\equiv 1/T$) is the inverse temperature, and the time dependent operator $O(t)$ is defined in the Heisenberg representation,

$$O(t) = e^{itH} O e^{-itH}. \tag{2.4}$$

Here, t denotes the time difference between two incident X-ray laser photons, and k_0 is the wave vector of them. After a small time interval Δ , these photons are

scattered out, respectively. k_1 and k'_1 are the wave vectors of the first and second outgoing photon.

Regarding H_{pf} as a perturbation, we separate Hamiltonian of Eq. (2.1) as,

$$H = H_0 + H_{pf}, \quad (2.5)$$

where

$$H_0 = H_p + H_f, \quad (2.6)$$

is treated as the unperturbed Hamiltonian. By expanding the time evolution operator in Eq. (2.4) with respect to H_{pf} ,

$$e^{-itH} \rightarrow e^{-itH_0} \left[1 - i \int_0^t d\tau \hat{H}_{pf}(\tau) + \dots \right], \quad (2.7)$$

we find that the lowest order terms which directly depend on t are of fourth order,

$$\begin{aligned} P(t) \rightarrow & \int_0^\Delta d\tau_1 \int_0^\Delta d\tau_2 \int_0^\Delta d\tau'_1 \int_0^\Delta d\tau'_2 \sum_{k_1, k'_1} \langle \langle a_{k_0} \hat{H}_{pf}(\tau'_1) e^{i\Delta H_0} a_{k_1}^\dagger \\ & \times e^{i(t-\Delta)H_f} a_{k_0} \hat{H}_{pf}(\tau'_2) e^{i\Delta H_0} a_{k'_1}^\dagger a_{k'_1} e^{-i\Delta H_0} \hat{H}_{pf}(\tau_2) a_{k_0}^\dagger e^{-i(t-\Delta)H_f} \\ & \times a_{k_1} e^{-i\Delta H_0} \hat{H}_{pf}(\tau_1) a_{k_0}^\dagger \rangle \rangle, \end{aligned} \quad (2.8)$$

where the operators with carets are defined in the interaction representation,

$$\hat{O}(\tau) = e^{i\tau H_0} O e^{-i\tau H_0}. \quad (2.9)$$

In Fig. 1, we present a diagrammatic analysis for the phonon-coupled scattering process corresponding to Eq. (2.8). In each diagram, the photons (phonons) are depicted by the wavy (dashed) lines, and the upper (lower) horizontal time lines stand for the bra (ket) vectors.¹⁵ Diagram (a) illustrates the changes of photon energy and wave number due to phonon emission and absorption, which corresponds to the well-known Stokes and anti-Stokes Raman scattering. Whereas, diagrams (b)-(e) represent the exchange, side band, rapid dumping and rapid exchange effects, respectively.

Obviously, diagram (c) bears no t -dependence, while diagrams (d) and (e) only contribute a substantial reduction to the time correlation between two laser pulses because of the duality of phonon interchange. Accordingly, the t -dependence is mainly determined by the diagrams (a) and (b). Allowing for this, the probability of interest can be written in the form as,

$$\begin{aligned} P(t) = & \int_0^\Delta d\tau_1 \int_0^\Delta d\tau_2 \int_0^\Delta d\tau'_1 \int_0^\Delta d\tau'_2 \frac{2V^4}{N^4} \sum_{q, q'} \langle \langle a_{k_0} e^{i\tau'_1 H_p} a_{k_0}^\dagger a_{k_0-q} \\ & \times e^{-i(\tau'_1-\Delta)H_p} a_{k_0-q}^\dagger a_{k_0} e^{i\tau'_2 H_p} a_{k_0}^\dagger a_{k_0+q} e^{-i(\tau'_2-\Delta)H_p} a_{k_0+q}^\dagger a_{k_0+q} \\ & \times e^{i(\tau_2-\Delta)H_p} a_{k_0+q}^\dagger a_{k_0} e^{-i\tau_2 H_p} a_{k_0}^\dagger a_{k_0-q} e^{i(\tau_1-\Delta)H_p} a_{k_0-q}^\dagger a_{k_0} e^{-i\tau_1 H_p} \\ & \times a_{k_0}^\dagger \rangle \rangle \langle \langle \hat{Q}_{q'}(\tau'_1) \hat{Q}_{q-q'}(\tau'_1) \hat{Q}_{-q+q'}(t+\tau'_2) \hat{Q}_{-q'}(t+\tau'_2) \hat{Q}_{q'}(t+\tau_2) \\ & \times \hat{Q}_{q-q'}(t+\tau_2) \hat{Q}_{-q+q'}(\tau_1) \hat{Q}_{-q'}(\tau_1) \rangle \rangle. \end{aligned} \quad (2.10)$$

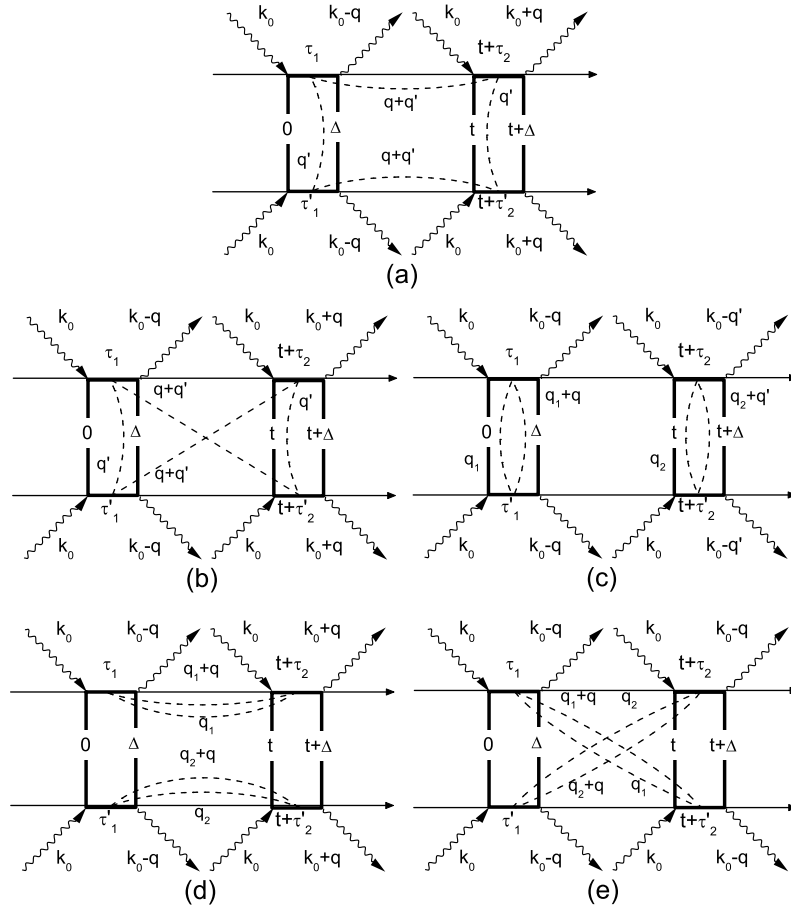


Fig. 1. Diagrammatic analysis for scattering process of photon with electric dipole moment (phonon). The photons and phonons are denoted by the wavy and dashed lines, respectively. In each diagram, the upper and lower horizontal time lines represent the bra and ket vectors, respectively.

Here, we note that the photon and phonon parts have been decoupled, and it can be easily seen that the origin of the t -dependence is nothing but the phonon (dipole) correlation.

In the case of forward X-ray scattering, we have $k_0 \approx k_1 \approx k'_1$, thus the normalized probability can be further simplified as,

$$\frac{P(t)}{P(0)} = \frac{\sum_{q,q'} |\langle\langle Q_q^2 \rangle\rangle G_{q+q'}(t)|^2}{\sum_{q,q'} |\langle\langle Q_q^2 Q_{q+q'}^2 \rangle\rangle|^2}, \quad (2.11)$$

where

$$G_q(t) = -2i\theta(t)\langle\langle \hat{Q}_q(t)\hat{Q}_{-q}(0) \rangle\rangle - 2i\theta(-t)\langle\langle \hat{Q}_{-q}(0)\hat{Q}_q(t) \rangle\rangle, \quad (2.12)$$

is the real time correlation function, or real time Green's function of phonon, and $\theta(t)$ is the step function. The Fourier component of this Green's function,

$$G_q(\omega) = \int_{-\infty}^{\infty} dt G_q(t) e^{-i\omega t}, \quad (2.13)$$

is related to the phonon spectral function [$\equiv A_q(\omega)$] through,¹⁶

$$\begin{aligned} \text{Re}G_q(\omega) &= \text{Re} \left[\frac{1}{2\pi} \int_{-\infty}^{\infty} d\omega' \frac{A_q(\omega)}{\omega - \omega' + i0^+} \right], \\ \text{Im}G_q(\omega) &= -\frac{1}{2} \coth \left(\frac{1}{2} \beta \omega \right) A_q(\omega). \end{aligned} \quad (2.14)$$

The phonon spectral function describes the response of lattice to the external perturbation, yielding profound information about dynamic properties of the crystal under investigation. Once we get the spectral function, the scattering probability and correlation function can be readily evaluated.

3. Numerical result and discussion

In the numerical calculation, we set phonon frequency $\omega_0=20$ meV, and make the parameters $c_4=0.076$, $c_6=0.00495$, $d_2=0.0967$. As indicated in Eq. (2.10), the t -dependence of probability is a result of phonon correlation. To reveal its relation with ferroelectric cluster dynamics, we start our discussion with an inspection on the property of phonon spectral function at the temperature regime $T \gtrsim T_c$. To this end, we first calculate the imaginary time Matsubara Green's function of phonon¹⁶ on a $12 \times 12 \times 12$ cubic lattice with a periodic boundary condition. This is done by a path integral Monte Carlo method.¹⁷ After obtaining the Matsubara function, we can derive phonon spectral function by the analytic continuation.^{16,17}

In Fig. 2, we plot the phonon spectral function in the paraelectric phase at different temperatures: (a) $T=T_c$, (b) $T=1.048T_c$, (c) $T=1.143T_c$ and (d) $T=1.429T_c$. In each panel, the spectra are arranged with wave vectors along the GXMR direction of Brillouin zone (see in the inset), and here ω refers to energy. Since the spectra are symmetric with respect to the origin $\omega=0$, in this graph we only show the positive part of them. When the temperature decreases toward T_c , as already well-known for the displacive type phase transition, the energy of phonon peak is gradually softened. In addition, a so-called central peak, corresponding to the low energy excitation of ferroelectric cluster, appears at the Γ point. On decreasing temperature, its intensity is dramatically enhanced, indicating that a stable dipole correlation of long-wave-length is built up. As mentioned above, the phonon spectral function can be understood as the optical response of dipole to the external perturbation. Therefore the collective excitation represented by the sharp resonant peak in spectra is nothing but the photon-created ferroelectric cluster.

The appearance of sharp peak near Γ point signifies that after excitation by soft X-ray, the photon-created ferroelectric clusters can be well preserved for a long relaxation time. Thus, they are likely to be observed by subsequent detective photons,

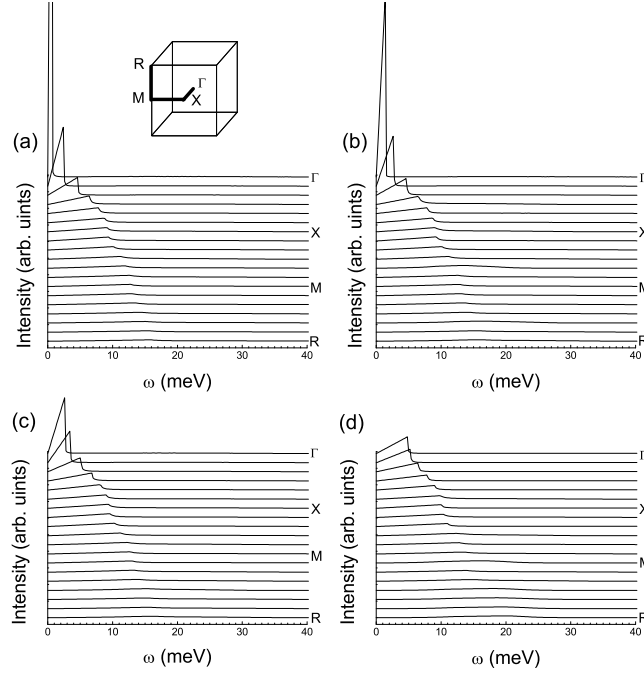


Fig. 2. Phonon spectral function along the line ΓXMR in the Brillouin zone at different temperatures of paraelectric phase: (a) $T=T_c$, (b) $T=1.048T_c$, (c) $T=1.143T_c$ and (d) $T=1.429T_c$. The inset of panel (a) shows the Brillouin zone with high symmetry lines.

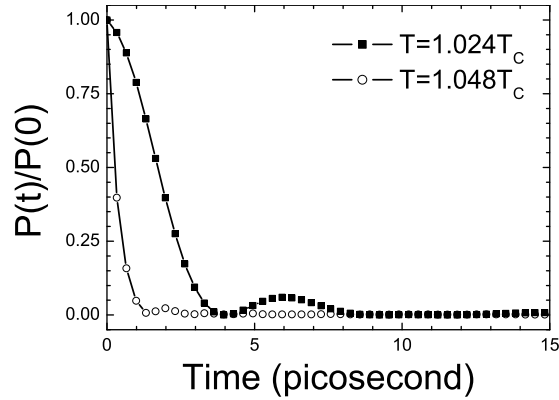


Fig. 3. Normalized speckle scattering probability as a function of time for paraelectric $BaTiO_3$, at $T=1.024T_c$ and $T=1.048T_c$.

resulting in a high intensity of speckle correlation. Keeping this in mind, we move on to the results of scattering probability. In Fig. 3, we show the normalized probability as a function of time at temperatures $T=1.024T_c$ and $T=1.048T_c$. From this figure,

we see in both cases, the probability declines exponentially with time, demonstrating that the photon-created clusters quickly disappear after the excitation and the system relaxes back to the paraelectric state. Meanwhile, at temperature closer to T_c , more gentle decay rate is observed, indicative of a critical slowing down of the relaxation time. This is because with the decrease of temperature, the intensity of local polarization is enhanced, and a long range correlation between dipole moments is to be established as well, making the relaxation of photon-created clusters slower and slower.

4. Summary

In conclusion, based on a coupled photon-phonon model, we conduct a theoretical survey on the relaxation dynamics of nano-sized ferroelectric cluster in the paraelectric phase of BaTiO₃, which is experimentally observed as a real time correlation of speckle pattern between two soft X-ray laser pulses. The density matrix is calculated by a perturbative expansion up to the fourth order terms, so as to characterize the time dependence of scattering probability. We show that this time dependence is determined by the relaxation dynamics of photo-created ferroelectric cluster, which is manifested as a central peak in the phonon spectral function. Near the T_c , cluster excitation is stable with a long relaxation time. While, at high temperature, it is suppressed by the thermal fluctuation, resulting in a short relaxation time. These features are in good agreement with Namikawa's experimental result.

Acknowledgments

This work is supported by the Next Generation Supercomputer Project, Nanoscience Program, MEXT, Japan.

References

1. D. L. Polla and L. F. Francis, Processing and characterization of piezoelectric materials and integration into microelectromechanical systems, *Annu. Rev. Mater. Sci.* **28** (1998) 563-597.
2. J. Harada, J. D. Axe, and G. Shirane, Neutron-scattering study of soft modes in cubic BaTiO₃, *Phys. Rev. B* **4** (1971) 155-162.
3. R. Migoni, D. Bauer, and H. Bilz, Origin of Raman scattering and ferroelectricity in oxidic perovskites, *Phys. Rev. Lett.* **37** (1976) 1155-1158.
4. B. Zalar, V. V. Laguta, and R. Blinc NMR evidence for the coexistence of order-disorder and displacive components in barium titanate, *Phys. Rev. Lett.* **90** (2003) 037601/1-4.
5. G. Völkel and K. A. Müller, Order-disorder phenomena in the low-temperature phase of BaTiO₃, *Phys. Rev. B* **76** (2007) 094105/1-8.
6. Y. Yamada, G. Shirane, and A. Linz, Study of critical fluctuations in BaTiO₃ by neutron scattering, *Phys. Rev.* **177** (1969) 848-857.

7. W. L. Mulvihill, K. Uchino, Z. Li and W. Cao, In-situ observation of the domain configuration during the phase transitions in barium titanate, *Phil. Mag. B* **74** (1996) 25-36.
8. G. K. H. Pang and K. Z. Baba-Kishi, Characterization of butterfly single crystals of BaTiO₃ by atomic force, optical and scanning electron microscopy techniques, *J. Phys. D* **31** (1998) 2846-2853.
9. J. W. Goodman, *Speckle Phenomena in Optics: Theory and Applications* (Roberts and Company, 2007).
10. R. Z. Tai, K. Namikawa, M. Kishimoto, M. Tanaka, K. Sukegawa, N. Hasegawa, T. Kawachi, M. Kado, P. Lu, K. Nagashima, H. Daido, H. Maruyama, A. Sawada, M. Ando, and Y. Kato, Picosecond snapshot of the speckles from ferroelectric BaTiO₃ by means of X-ray lasers, *Phys. Rev. Lett.* **89** (2002) 257602/1-4.
11. R. Z. Tai, K. Namikawa, A. Sawada, M. Kishimoto, M. Tanaka, P. Lu, K. Nagashima, H. Maruyama, and M. Ando, Picosecond view of microscopic-scale polarization clusters in paraelectric BaTiO₃, *Phys. Rev. Lett.* **93** (2004) 087601/1-4.
12. K. Namikawa, unpublished.
13. J. A. Krumhansl and J. R. Schrieffer, Dynamics and statistical mechanics of a one-dimensional model Hamiltonian for structural phase transitions, *Phys. Rev. B* **11** (1975) 3535-3545.
14. A. N. Rubtsov and T. Janssen, Quantum phase transitions in the discrete φ^4 model: The crossover between two types of transition, *Phys. Rev. B* **63** (2001) 172101/1-4.
15. K. Nasu, Resonance enhancement of inelastic X-ray scatterings induced by strong visible lights, *J. Phys. Soc. Jpn.* **63** (1994) 2416-2427.
16. A. Fetter and J. Walecka, *Quantum Theory of Many-Particle Systems* (MacGraw Hill, New York, 1971).
17. K. Ji, H. Zheng, and K. Nasu, Path-integral theory for evolution of momentum-specified photoemission spectra from broad Gaussian to two-headed Lorentzian due to electron-phonon coupling, *Phys. Rev. B* **70** (2004) 085110/1-9.